

## KINEMATICS FOR A ROUGH TERRAIN MOBILE ROBOT TO CLIMB UP A STEP

SHURO NAKAJIM

*The Dept. of Advanced Robotics, Chiba Institute of Technology,  
Narashino, Chiba 275-0016, Japan*

*Email: shuro.nakajima@it-chiba.ac.jp,  
www.nakajima-lab.it-chiba.ac.jp*

The rough terrain mobile robot "RT-Mover", which is a leg-wheel-type robot built of very simple mechanism, can move on continuous rough terrain.<sup>1</sup> However, in a real environment there is also discontinuous rough terrain, where it can not get about. The step-up gait for an upward step has been studied to walk on discontinuous rough terrain. In this paper, a flow of the step-up gait is introduced. After that, kinematics to climb up a step is discussed in detail, and is evaluated through simulation and experiment.

*Keywords:* Kinematics, Rough Terrain, Step-up Gait, Leg-wheel Robot, Wheeled Robot, Moving Strategy

### 1. Introduction

There is a strong demand for mobile robots that can move on rough terrain in various applications, for example, to aid people who have difficulty in walking. However, few robots are suitable for use in rough terrain at practical level. On the other hand, many rough terrain mobile robots at research level exist. Most of them are classified into the following three categories.

1) Legged robots: These have excellent mobility with high stability; legs are used to support the body and maintain its stability. The mobility of those has been extensively studied, e.g. the TITAN series.<sup>2</sup>

2) Wheeled robots: These are most commonly selected for traversing continuous surfaces that include rough terrain. Because of their stability and simple controls etc., wheel mechanism is the most frequently used for exploration rovers. Among examples of wheeled mobile robots, Micro5<sup>3</sup> has passive linkage mechanisms, and SpaceCat<sup>4</sup> has active linkage mechanisms.

3) Wheeled legged robots: These have the merits of both legs and wheels. Work Partner<sup>5</sup> is equipped with wheels placed at the ends of the legs. Chariot 3<sup>6</sup> has separate wheels and legs.

Although a legged mechanism is highly mobile on rough terrain, it is complex. On the other hand, most of wheeled robots cannot travel over discontinuous terrain; however, they are usually the best solution for continuous terrain. A hybrid mechanism provides the strengths of both wheels and legs, although such mechanisms also tend to be complex.

RT-Mover<sup>1</sup> has a simple mechanism and enough mobility for the following target environments: 1. An indoor environment with an uneven ground surface, 2. An artificial outdoor environment with an uneven ground surface and a staircase, and 3. Natural terrain such as a trail in a forest. Its mechanism is different from those of conventional mobile robots. Four wheels are mounted at the tip of every leg, and the leg mechanism is quite simple (Fig.1). RT-Mover has four active wheels and only five active shafts, and it can move on discontinuous rough terrain while maintaining a sheet-like body horizontally. It can move like a wheeled robot and also walk over a step like a legged robot, despite the simplicity of the mechanism.

In this paper, a step-up gait for an upward step is discussed. The flow of processes in the step-up gait is introduced, and the kinematics during the gait in detail is proposed. It is then evaluated through simulation and experiment.

## 2. RT-Mover

Fig.1 shows RT-Mover, the four-wheel-type mobile robot built for rough terrain with a simple leg mechanism. It has four driving wheels, front and rear steering shafts, front and rear roll-adjustment shafts, and a seat pitch adjustment shaft at the center of its body. RT-Mover is equipped with sensors: an encoder and a current sensor for each joint motor, and posture angle sensors relative to its seat part (pitch and roll).

The robot is characterized by the smallest number of driving shafts that assist its movement on discontinuous rough terrain while maintaining its seat part in a horizontal plane, where an occupant or load is seated. Other than the wheels, it has only five degrees of freedom in total. In reference,<sup>1</sup> I showed that RT-Mover can move on continuous rough terrain while maintaining the seat part in a horizontal plane by applying eq. (1) to the pitch adjustment shaft and each front and rear roll-adjustment shaft (basic movement control method).

$$T_d = K(\theta_d - \theta) + D(\dot{\theta}_d - \dot{\theta}) = -K\theta - D\dot{\theta}, \quad (1)$$

$T_d$ : target torque;  $\theta$ : seat part's posture angle;  $\theta_d$ : seat part's target posture angle ( $=0$ );  $K$  and  $D$ : angle gain and angular velocity gain.

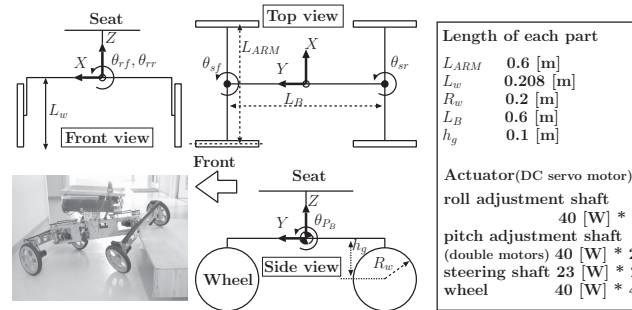


Fig. 1. The rough terrain mobile robot RT-Mover

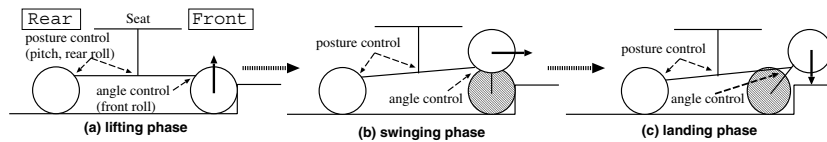


Fig. 2. An upward step

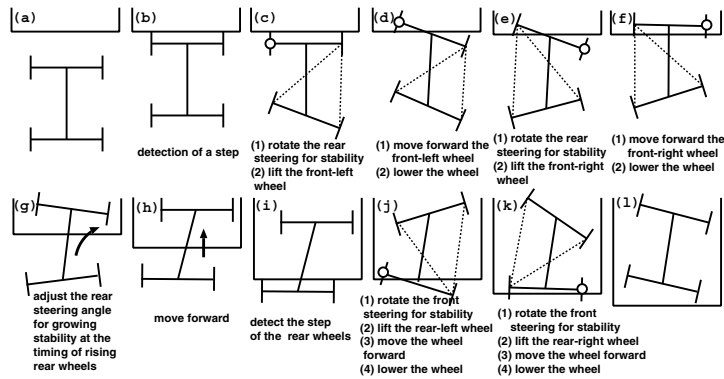


Fig. 3. Flow of processes in the step-up gait

### 3. Step-up Gait Strategy

Using the control method in eq. (1), RT-Mover can move on rough terrain while maintaining its posture and its wheels can be in continuous contact with the ground. However, with large steps or gaps, the ground contact points of the wheels need to be altered by lifting the wheels. In this study, I discuss a step-up moving method as the first step of studying a moving method on discontinuous rough terrain. I now consider a case of lifting a wheel onto a step on which the wheel cannot move (Fig.2).

Assuming that static stability is maintained during the movement, a wheel is lifted like a leg while constantly supporting the body on at least three points in order to position the center of gravity on a supporting polygon. Since the robot cannot move its center of gravity without altering the supporting points due to its small degree of freedom, the position of the supporting point is adjusted by rotating the steering shafts in order to maintain static stability. Of the three supporting points, since the steering shaft on the wheel-lifting side (leg-side steering) is used for moving the lifted wheel forward, static stability is increased by rotating the steering shaft of the other side (support-side steering) (for example, Fig.3(c)). Since the left-right order does not affect the movement in the step shown in Fig.2, the robot can move onto the step by lifting the wheels one by one in the order front-left, front-right, rear-left, and rear-right (Fig.3).

The step-up gait which is also statically stable shall be proposed in another paper.<sup>7</sup> This gait was confirmed theoretically and practically to be capable of maintaining static stability while climbing a step up to 0.2 [m] in height, when given steering support to increase stability up to a maximum angle of 30 [°].

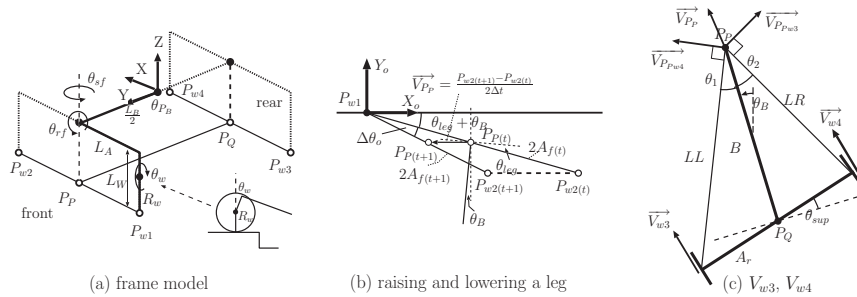


Fig. 4. Model for analysis

4. Study of Trajectory

In the below analysis, I use a “projection frame” (Fig.4(a)), which comprises projecting line segments connecting the wheel landing points (arms) and a line segment connecting the centers of the arms (body) to horizontal planes. I take a right-handed coordinate system with the center of the projection frame as the origin, the direction of travel is defined as Y and the vertical axis as Z, such that the following matrix  ${}^0T_{wfl}$  maps coordinates with the front-left leg at the origin to the body-centered coordinate system:

$$\begin{aligned}
{}^0T_{w_{fl}} = & \begin{pmatrix} 1 & 0 & 0 & 0 \\ 0 & C\theta_p & -S\theta_p & 0 \\ 0 & S\theta_p & C\theta_p & 0 \\ 0 & 0 & 0 & 1 \end{pmatrix} \begin{pmatrix} 1 & 0 & 0 & 0 \\ 0 & 1 & 0 & \frac{LB}{2} \\ 0 & 0 & 1 & 0 \\ 0 & 0 & 0 & 1 \end{pmatrix} \begin{pmatrix} C\theta_{sf} & -S\theta_{sf} & 0 & 0 \\ S\theta_{sf} & C\theta_{sf} & 0 & 0 \\ 0 & 0 & 1 & 0 \\ 0 & 0 & 0 & 1 \end{pmatrix} \begin{pmatrix} C\theta_{rf} & 0 & S\theta_{rf} & 0 \\ 0 & 1 & 0 & 0 \\ -S\theta_{rf} & 0 & C\theta_{rf} & 0 \\ 0 & 0 & 0 & 1 \end{pmatrix} \\
& \begin{pmatrix} 1 & 0 & 0 & -L_A \\ 0 & 1 & 0 & 0 \\ 0 & 0 & 1 & 0 \\ 0 & 0 & 0 & 1 \end{pmatrix} \begin{pmatrix} 1 & 0 & 0 & 0 \\ 0 & 1 & 0 & 0 \\ 0 & 0 & 1 & -L_r \\ 0 & 0 & 0 & 1 \end{pmatrix} \begin{pmatrix} 1 & 0 & 0 & 0 \\ 0 & C\theta_w & -S\theta_w & 0 \\ 0 & S\theta_w & C\theta_w & 0 \\ 0 & 0 & 0 & 1 \end{pmatrix} \begin{pmatrix} 1 & 0 & 0 & 0 \\ 0 & 1 & 0 & 0 \\ 0 & 0 & 1 & -R \\ 0 & 0 & 0 & 1 \end{pmatrix} \quad (2)
\end{aligned}$$

#### 4.1. Lifting and Landing Phase

When lifting or landing the front-right wheel, a velocity command value will be set for the front roll-adjustment shaft. In order to avoid contacting the step lateral surface, the wheel is moved up and down without moving back or forth. As will be stated in the next chapter, the posture control in eq. (1) is applied to pitch adjustment and rear roll-adjustment shafts, and rotation of the lifted front-right wheel and the supporting front-left wheel is stopped. In order to widen the supporting polygon, the rear steering shaft is rotated to its steering limit. The control parameters of the front steering shaft, the rear-left wheel, and the rear-right wheel are determined by the value set for the front roll-adjustment shaft.

Now I explain how to derive these control parameters. As shown in Fig.4(b), I discuss it on an absolute coordinate system with its origin at the landing position of the front-left wheel ( $P_{w1}$ ). In Fig.4(b), I assume the position of the front-right wheel ( $P_{w2}$ ) when moving the front roll-adjustment shaft for a small amount of time  $\Delta t$ , at a velocity of  $P_P$  and a small angle  $\Delta\theta_o$ , and derive the angular velocity of the front steering shaft  $\dot{\theta}_{sf}$  and the velocities of the rear-left and rear-right wheels  $\vec{V}_{w3}$  and  $\vec{V}_{w4}$ . Since the wheel is moved up and down without moving in the Y direction, the Y coordinate of  $P_P$  is constant.

$A_{f(t)}$  is the distance between  $P_{w1(t)}$  and  $P_{P(t)}$ ; since this is half the distance between  $P_{w1(t)}$  and  $P_{w2(t)}$ , it may be derived from eq. (2). From this equation,  $A_{f(t)}$  depends on the front steering  $\theta_{sf}$ , front roll axis  $\theta_{rf}$  and body pitch.  $A_{f(t+1)}$  is the value of  $A_f$  after a small incremental movement of  $\theta_{rf}$ . Since it is difficult to solve analytically,  $\theta_{sf}$  and  $\theta_{PB}$  are approximated as not varying with time t. Since the Y axis moves in a fixed up and down path, the Y coordinate of  $P_{w2}$  is fixed and is given below.

$$(P_{w2x(t)}, P_{w2y(t)}) = (2A_{f(t)} \cos(\theta_{leg} + \theta_B), 2A_{f(t)} \sin(\theta_{leg} + \theta_B)) \quad (3)$$

$$(P_{w2x(t+1)}, P_{w2y(t+1)}) = (\sqrt{4A_{f(t+1)}^2 - P_{w2y(t)}^2}, P_{w2y(t)}) \quad (4)$$

The velocity of  $P_P$  ( $\overrightarrow{V_{P_P}}$ ) and small velocity angle  $\Delta\theta_o$  are obtained below by eqs. (3) and (4).

$$\overrightarrow{V_{P_P}} = (V_{P_{Px}}, V_{P_{Py}}) = \left( \frac{P_{w2x(t+1)} - P_{w2x(t)}}{2\Delta t}, 0 \right) \quad (5)$$

$$\Delta\theta_o = -\tan^{-1} \frac{P_{w2y(t)}}{P_{w2x(t)}} - \tan^{-1} \frac{P_{w2y(t+1)}}{P_{w2x(t+1)}} \quad (6)$$

$\Delta\theta_o$  is the sum of the changes in the projected front steering angle  $\theta_{leg}$  and body rotation  $\theta_B$ ,  $\Delta\theta_o = \Delta\theta_{leg} + \Delta\theta_B$ . Among these variables, the one that includes the control parameter of the front steering shaft is  $\dot{\theta}_{leg}$ , and the control parameter of the front steering is determined by calculating  $\dot{\theta}_B$  and the relationship between  $\dot{\theta}_{leg}$  and  $\dot{\theta}_{sf}$ . The relationship between  $\dot{\theta}_{leg}$  and  $\dot{\theta}_{sf}$  is determined topologically from the relations below.  $\theta_{P_B}$  is obtained from attitude sensor information on the seat part and the pitch adjustment angle.

$$\theta_{leg} = \theta_{sf} \cos \theta_{P_B} + \theta_{rf} \sin \theta_{P_B}, \quad (7)$$

$$\therefore \dot{\theta}_{sf} = \frac{\dot{\theta}_{leg} - \dot{\theta}_{rf} \sin \theta_{P_B} + \dot{\theta}_{P_B} (\theta_{sf} \sin \theta_{P_B} - \theta_{rf} \cos \theta_{P_B})}{\cos \theta_{P_B}}. \quad (8)$$

The angle velocity of the body rotation  $\dot{\theta}_B$  is obtained as given below, where  $B$  is the length of the projection body and  $V_{P_{Qx}}$  is derived from the velocity of the rear-right and rear-left wheels as subsequently described.

$$\dot{\theta}_B = \frac{V_{P_{Qx}} - V_{P_{Px}}}{B} \quad (9)$$

#### 4.1.1. Control Amounts of Rear-Left and Rear-Right Wheels

The velocities of the rear-left and rear-right wheels,  $\overrightarrow{V_{w3}}$  and  $\overrightarrow{V_{w4}}$ , are derived. In Fig.4(c), taking the velocities gained by point  $P_P$  gains from the velocities of the rear wheels as  $\overrightarrow{V_{P_{Pw3}}}$  and  $\overrightarrow{V_{P_{Pw4}}}$ , the velocity of  $P_P$  is

$$\overrightarrow{V_{P_P}} = \overrightarrow{V_{P_{Pw3}}} + \overrightarrow{V_{P_{Pw4}}}. \quad (10)$$

The relationship between  $\overrightarrow{V_{w3}}$  and  $\overrightarrow{V_{P_{Pw3}}}$ , for example, is given by  $|\overrightarrow{V_{w3}}| = \frac{2A_r}{LR} |\overrightarrow{V_{P_{Pw3}}}|$ , where  $LR$  is obtained from  $B(t)$ . In addition, since body length  $B$  also varies with  $\theta_{P_B}$ , it is also necessary to include this change  $(B_{(t+1)} - B_{(t)})/\Delta t$  in the calculation of  $\overrightarrow{V_{w3}}$  and  $\overrightarrow{V_{w4}}$ , as given below.

$$|\overrightarrow{V_{w3}}| = \frac{2A_r}{LR} |\overrightarrow{V_{P_{Pw3}}}| + \dot{B}, \quad |\overrightarrow{V_{w4}}| = \frac{2A_r}{LL} |\overrightarrow{V_{P_{Pw4}}}| + \dot{B}. \quad (11)$$

$B_{(t+1)}$  and  $B_{(t)}$  are calculated from coordinates of  $P_P$  and  $P_Q$ , obtained in the same way from eq. (2).

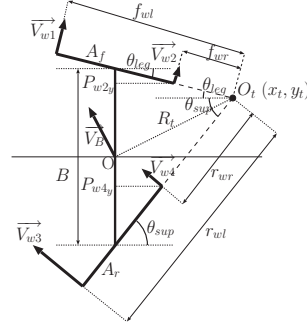
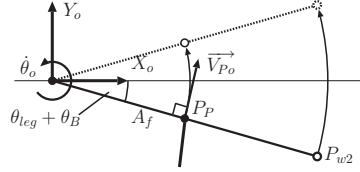


Fig. 5. Calculation model for swinging Fig. 6. Calculation model for wheel mode phase

**4.2. Swing Phase**

Fig.5 is a model of the swing phase, wherein the origin of the absolute coordinate system is the front-left wheel and the lifted leg is represented by the front-right wheel. The trajectory is set such that point  $P_P$  draws a circular path around the front-left wheel. Velocities of the front steering shaft and rear wheels are determined such that they satisfy  $\vec{V}_{P_P}$ . Letting  $\vec{V}_{P_P}$  be the set value that gives the angular velocity  $\dot{\theta}_o$ , I obtain the below:

$$|\vec{V}_{P_P}| = A_f |\dot{\theta}_o|, \quad \vec{V}_{P_P} = (-|\vec{V}_{P_P}| \sin(\theta_{leg} + \theta_B), |\vec{V}_{P_P}| \cos(\theta_{leg} + \theta_B)). \quad (12)$$

With the velocity of point  $P_P$  determined, as in the lifting and landing phases, the control parameter of the front steering adjustment shaft and velocities of the rear wheels can be obtained.

**4.3. Wheel mode**

In Fig.3(g)-(h), the robot moves with all four wheels supporting the body. Since the velocity of the body center,  $V_B$ , and front and rear steering axes,  $\theta_{leg}$  and  $\theta_{sup}$ , are given as parameters, I derive the desired wheel velocities with no slipping,  $\vec{V}_{w1} \sim \vec{V}_{w4}$ . Taking the center of turning axis of the robot  $O_t = (x_t, y_t)$  and a turning radius  $R_t$ , the angular velocity  $\omega_B$  is given by  $\omega_B = |V_B|/R_t$ . Since each wheel rotates about  $O_t = (x_t, y_t)$  with an angular velocity  $\omega_B$ ,  $|\vec{V}_{w1}|$  is for example given by  $|\vec{V}_{w1}| = f_{wl} \omega_B$ . Hence if  $R_t, f_{wl}, f_{wr}, r_{wl}$  and  $r_{wr}$  are known, the velocity of each wheel is known. Except under conditions such as  $|\theta_{leg}| = |\theta_{sup}|$  where front and rear steering angles are equal and the turning radius becomes infinite, the topology in Fig.6 leads to the relation below, and  $R_t$  can be obtained from  $R_t = \sqrt{x_t^2 + y_t^2}$ .

$$(x_t, y_t) = \left( \frac{B}{\tan \theta_{sup} - \tan \theta_{leg}}, \frac{B \tan \theta_{sup} + \tan \theta_{leg}}{2 \tan \theta_{sup} - \tan \theta_{leg}} \right) \quad (13)$$

Variables such as  $f_{wl}$  are obtained in the form  $f_{wl} = |x_t - P_{w1x}| / \cos \theta_{leg}$ . However, under the condition  $|\theta_{leg}| = |\theta_{sup}|$ ,  $V_{wi} = V_B (i = 1 \sim 4)$ .

## 5. Evaluation by Simulation and Experiment

The proposed trajectory was derived by using some approximate values, so the degree of errors is evaluated below. Fig.7 shows the position of the front-left wheel along the Y and Z axes when the initial position of the front steering  $\theta_{sf}$  is 20 [°] and the rear steering  $\theta_{sr}$  is -30 [°], letting the front-left wheel be the lifted leg with the front roll-adjustment shaft rotated at an angular velocity  $\dot{\theta}_{rf} = 0.1$  [rad/s] and  $\dot{\theta}_o$  in the swing phase is 0.1 [rad/s], leg lifting height is 0.15 [m], and distance along the Y axis in the swing phase is 0.15 [m]. These conditions are chosen in order to confirm the degree of errors under the conditions that can be affected by approximation and are within the usable range. Lifting occurred between 0 [s] and 3.7 [s] and landing between 6.5 [s] and 10 [s]. Although there is an error of at most 0.007 [m] during lifting and landing, the leg moved up and down while almost maintaining a constant Y coordinate. As for the Z coordinate, the leg moves up to 0.15 [m] in height and shifts to the swing phase between 0 [s] and 3.7 [s]. The reason for increase in leg height between 3.7 [s] and 6.5 [s] is the constant position maintained by the front roll-adjustment shaft during the swing phase, which changes the body pitch angle with a change in the front steering angle and causes the leg height to increase.

Fig.7(c) shows the effect on the Z direction in an experiment performed under the same conditions as the simulation. Fitting LEDs to the lifted wheel, a camera was used to photograph the movement at shutter-speed intervals. It can be seen that movement can be made in the up-down direction with the Y coordinate maintained at an approximate constant. Fig.7 thus demonstrates movement along the desired trajectory.

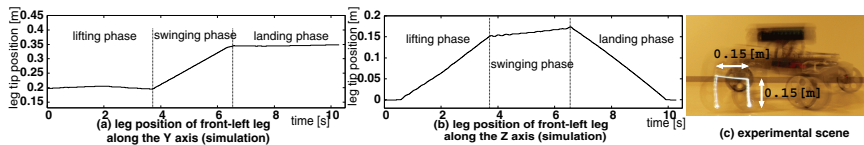


Fig. 7. Leg trajectory



Fig. 8. A trial experiment (step-up gait)

## 6. Conclusion and Future Work

This research presents the kinematics during the step-up gait. The gait enables the mobile robot RT-Mover, which only has 5 driving shafts other than 4 driving wheels, to move up onto a step while maintaining the seat part on a horizontal plane by means of a simple leg mechanism. I calculated approximate trajectories for each wheel lifting, moving forward, and landing, and also calculated the trajectories to allow the wheels to proceed forwards while adjusting the body rotation. I evaluated the proposed kinematics through the simulation and the experiment. Fig.8 shows the experiment to test a step-up gait using the proposed kinematics discussed. It is demonstrated that by using the wheels as legs, it is now possible to climb steps of 0.1 [m] height which could not previously be negotiated. Subsequent work will propose the step-up gait outlined in this paper, and seek to improve mobility of the RT-Mover.

## Acknowledgement

This work was supported by Kazuhisa Ietomi, a senior student of our laboratory. I would like to express my gratitude for his support.

## References

1. S. Nakajima, "Concept of a Four-wheel-type Mobile Robot for Rough Terrain RT-Mover" Proc. of the IROS, pp.3257-3264, 2009.
2. S. Hirose, et al., "The Gait Control System of the Quadruped Walking Vehicle", Journal of the Robotics Society of Japan, vol.3, no.4, pp.304-323, 1985.
3. T. Kubota, et al., "Small, light-weight rover "Micro5" for lunar exploration", Acta Astronautica, 52, 447-453, 2003.
4. M. Lauria, et al., "Design and control of an innovative micro-rover", Proc. of the ESA Workshop on Advanced Space Technologies for Robotics and Automation, 1998.
5. I. Leppanen, "Workpartner-HUT automations new hybrid walking machine", Proc. of the CLAWAR'98, 1998.
6. S. Nakajima, et al., "Adaptive Gait for Large Rough Terrain of a Leg-wheel Robot", Journal of Robotics and Mechatronics, vol.21, no.3, pp.419-426, 2009.
7. S. Nakajima, "Proposal for Step-up Gait of RT-Mover, A Four-Wheel-Type Mobile Robot for Rough Terrain with Simple Leg Mechanism", IROS 2010, now submitting.